

MgO/Fe(100) interface: A study of the electronic structure

L. Plucinski,* Y. Zhao, and B. Sinkovic

Department of Physics, University of Connecticut, Storrs, Connecticut 06269, USA

E. Vescovo

National Synchrotron Light Source, Brookhaven National Laboratory, Upton, New York 11973, USA

(Received 3 December 2006; revised manuscript received 1 April 2007; published 6 June 2007)

Epitaxial MgO(100) films, deposited on the Fe(100) surface by direct evaporation of stoichiometric magnesium oxide under ultrahigh-vacuum conditions, are examined by spin-polarized valence-band photoemission and magnetic linear dichroism in core-level spectroscopy. The excellent quality of the MgO films prepared in this way is clearly revealed by relatively small photocurrent intensity observed above the MgO valence-band maximum and by spectral features in the photoemission data. No evidence of the formation of an interfacial FeO layer is found in this MgO/Fe(100) system. Only a structural reordering is promoted by annealing the interface up to 400 °C, as evident by the minute changes in the photoemission spectra. Further annealing to 500 °C, however, leads to more substantial changes in the spectra, possibly related to further ordering of the interface and/or partial uncovering of the Fe(100) metal due to MgO desorption and/or clustering. The influence of screening effects from the Fe(100) substrate to the photohole created by the photoemission process in the MgO overlayer is also examined.

DOI: [10.1103/PhysRevB.75.214411](https://doi.org/10.1103/PhysRevB.75.214411)

PACS number(s): 75.70.-i, 79.60.-i, 68.35.-p

I. INTRODUCTION

In recent years, there have been significant advances in the preparation of single crystalline magnetic tunnel junctions (MTJs) based on MgO(100) insulating barriers. For example, the theoretically predicted tunneling magnetoresistance (TMR) of several hundred percent^{1,2} in Fe/MgO/Fe(100) has been experimentally verified with values of 180–220 % for room temperature (Refs. 3 and 4) and higher values are being reported for various other electrode compositions.^{5–7}

The exact composition and atomic structure at the barrier/ferromagnet interface are of primary importance for the performance of single crystalline MTJs. In the case of MgO/Fe(100), surface x-ray diffraction measurements⁸ suggest the existence of a partial interfacial FeO layer, which could strongly reduce the Fe spin polarization at the interface and, therefore, negatively influence the performance of the MTJ.⁹ Other studies¹⁰ find no interfacial FeO layer, and also when the second interface is formed, i.e., Fe is deposited on MgO(100), such an oxide layer is clearly absent.^{11,12} Thus, an FeO layer does not appear to be an intrinsic property of the interface. This view is also supported by theoretical calculations by Li and Freeman,¹³ which find little interaction between a thin Fe(100) layer and the MgO(100) substrate. Similarly, recent total energy calculations of Yu and Kim¹⁴ also find that no formation of interfacial FeO is preferred under Mg-rich conditions.

Manipulating the composition of the electrodes and improving the crystalline structure at the ferromagnet-barrier interface are keys to fabricating alternative devices with higher TMR. A considerable effort, theoretical as well as experimental, is currently underway to investigate this topic. Most notably, recent theoretical calculations suggest placing a thin layer of Au (Ref. 15) or Ag (Ref. 16) in between the ferromagnetic electrode (Fe) and the insulating barrier

(MgO), as an effective way to prevent oxidation of the ferromagnet, thus preserving its large spin polarization at the interface. Large enhancements of the TMR effect (up to 1000%) are calculated for these ferromagnet/noble metal/barrier systems, assuming ideal interfaces. On the other hand, experimental work indicates that annealing up to 400 °C leads to substantial improvements in the magnetoresistance of the “simple” Fe/MgO/Fe(100) tunnel junctions prepared at room temperature.^{3,6,7,17} The characterization of the MgO/Fe interface is, therefore, an important and timely issue.

Spin- and angular-resolved photoemissions are particularly suited for characterization of these MTJ systems. Indeed, the electronic structure at the MgO/Fe(100) interface has already been probed by this technique. Valence-band spectra in the submonolayer and up to 1 ML (monolayer) MgO coverage have been reported in the photon energy range between 35 and 60 eV for MgO films prepared by depositing metallic Mg in the presence of an oxygen atmosphere.¹⁸ Furthermore, soft x-ray spin-polarized photoemission spectra, which represent the density of states, of 2 ML MgO/Fe(100) grown on bulk MgO(100) were presented by Sicot *et al.*^{19,20} More recently, a study combining spin-polarized photoemission, diffraction, and microscopy of MgO grown on another low index Fe surface, Fe(110),²¹ revealed the existence of an interfacial FeO layer for the MgO/Fe(110) interface. However, the MgO films in this study were grown by exposing the Fe(110) surface to Mg vapors in a controlled oxygen atmosphere at room temperature (RT),²² similar to the method used in Ref. 18.

In the present study, valence-band spin-polarized photoemission spectra and core-level magnetic linear dichroism spectra are presented for the MgO/Fe(100) system for MgO thicknesses between 0.5 and 10 ML. Moderately high incident photon energy ($h\nu=128$ eV) is used to minimize surface contributions and simultaneously excite valence bands

and shallow Fe 3*p* and Mg 2*p* core levels. The MgO/Fe(100) junction is prepared at RT by direct evaporation of stoichiometric MgO onto the clean Fe(100) surface under ultrahigh-vacuum conditions (UHV). In this way, it is less likely to form the FeO layer at the MgO/Fe(100) interface, which we confirm by the combined analysis of valence-band and core-level spectra. Furthermore, in view of reported postannealing enhancement of TMR mentioned above,^{3,6,7,17} the stability of the MgO/Fe(100) interface upon annealing has been investigated. Annealing up to 400 °C produces only atomic reordering of the interface as evidenced by the small modifications in the photoemission spectra, mostly a sharpening of all spectral features. More substantial modifications of the spectra are instead observed by annealing to 500 °C. These higher-temperature changes are possibly related either to further ordering of the interface or to the desorption and/or clustering of MgO.

Additionally, an interesting dynamic property of the electronic structure of the MgO/Fe interface is discussed. The response of the conduction electrons from the Fe side of the interface to the photohole creation in the thin MgO layers is observed as additional screening in photoemission spectra.

II. EXPERIMENT

Experiments were performed at beamline U5UA at the National Synchrotron Light Source (NSLS). This beamline is equipped with a planar undulator and a spherical grating monochromator.²³ The photon beam covers the range 20–200 eV and is highly linearly polarized in the horizontal plane.

A commercial hemispherical electron energy analyzer,²⁴ originally equipped with seven channeltrons, has been modified to host a mini-Mott spin polarimeter,²⁵ leaving three channeltrons for standard high-resolution spin integrated photoemission. The analyzer was set to the angular-resolved mode ($\pm 1^\circ$ angular acceptance). The experiments were performed in normal emission with the photon beam incident at 45° with respect to the sample normal. Typical overall resolution was 150 meV for spin-integrated and 300 meV for spin-polarized spectra.

A Mo(100) single crystal was chosen as the substrate. It was mounted on an UHV compatible manipulator with the [001] direction vertical and cleaned by repeated flashing to 2000 °C. The sample temperature was monitored by a W-Rh thermocouple attached directly to the Mo(100) crystal.

Fe(100) films of 40 Å thickness were grown at RT at the rate of 5 Å/min by electron-beam evaporation. The base pressure in the chamber was 5×10^{-11} Torr and rose to about

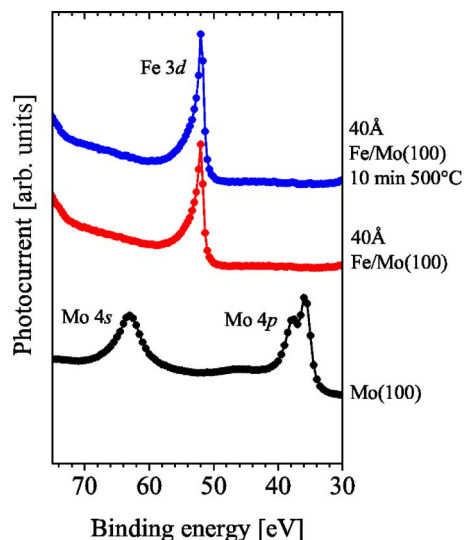


FIG. 1. (Color online) Survey photoemission spectra in the region of Mo 4*s*, Mo 4*p*, and Fe 3*d* core levels. The annotations are printed in figure.

1×10^{-10} Torr during Fe depositions. We are not aware of any *in situ* UHV study of Fe growth on Mo(100) in the coverage region thicker than a few monolayers,²⁶ although Mo(100) single-crystal substrates were successfully used to grow sophisticated Fe/Mo multilayer structures.²⁷ Our low-energy electron-diffraction (LEED) observations indicate that above a few monolayers, the growth proceeds epitaxially with a relaxed bulk Fe lattice constant. This behavior is essentially identical to that found in the similar Fe/W(100) system²⁸ (Mo and W have the same bcc structure and very similar lattice constants, $a_{\text{Mo}}=3.147$ Å, $a_{\text{W}}=3.165$ Å).

The preparation of atomically flat Fe(100) films requires special precautions. We have found improvements in the photoemission spectra (sharpening of the features) and LEED patterns of Fe films upon annealing the sample to 500 °C for approximately 10 min, and such annealed Fe(100) films were used for subsequent MgO deposition. Figure 1 presents spectra of Fe/Mo(100) films before and after annealing to 500 °C in comparison with the spectrum of clean Mo(100). There is no indication of Mo core levels in the Fe/Mo(100) spectrum after annealing, which excludes the model with 2 ML wetting layer and three-dimensional islands.^{29,30}

MgO was deposited at the slow rate of approximately 0.2 Å/min from pieces of stoichiometric MgO single crystals put into a tungsten crucible and heated by electron-beam bombardment. The coverage thicknesses were estimated by calibrating the evaporator *in situ* with a quartz balance and

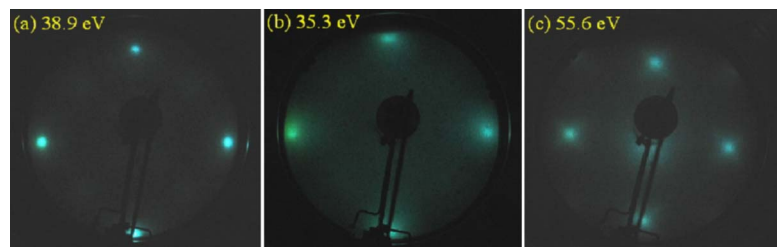


FIG. 2. (Color online) LEED patterns for (a) clean Fe(001), (b) 1 ML MgO/Fe(001), and (c) 10 ML MgO/Fe(001).

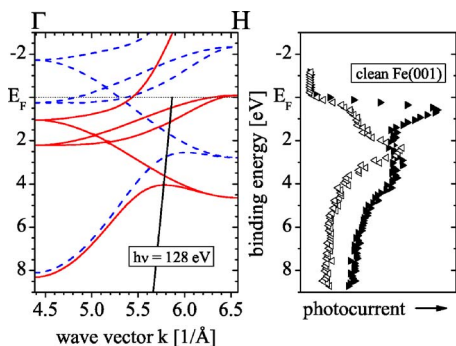


FIG. 3. (Color online) Left panel: bulk band structure of Fe along the Γ - H high-symmetry direction calculated using WIEN2K (Ref. 49). Solid and dashed lines represent majority and minority spin bands, respectively. The energy distribution curve appropriate for $h\nu=128$ eV (assuming direct transitions, free-electron final states, and inner potential $V_0=10$ eV) is superimposed on the band-structure calculation. Right panel: spin-polarized photoemission spectrum taken at $h\nu=128$ eV in normal emission. \blacktriangleright , majority spin; \blacktriangleleft , minority spin.

further confirmed by comparisons to previous studies.¹⁸ MgO films are known to grow pseudomorphically in a layer-by-layer fashion on the Fe(100) surface up to about 6 ML (Ref. 31), while the thickness of the barrier in the optimized MTJs is between 5 and 15 ML.^{3,4} 1 ML of MgO corresponds to approximately 2.2 Å thickness.³² The epitaxial growth mode of the MgO(100) overlayers on Fe(100)/Mo(100) is confirmed in the LEED patterns displayed in Fig. 2. While these LEED patterns are not as sharp as those from MgO overlayers grown on Fe whiskers,³¹ they do show fourfold satellite spots, surrounding each (10) LEED beam, in good agreement with previous observations. These satellite spots are clearly visible at high MgO coverage [see LEED picture for 10 ML MgO, Fig. 2(c)] and are related to misfit dislocations.³¹

III. RESULTS AND DISCUSSION

A. Valence-band measurements

In Fig. 3, a portion of the bulk band structure of Fe is compared with the spin-resolved photoemission spectrum measured from the clean Fe(100) surface in normal emission with photon energy $h\nu=128$ eV. In normal emission geometry, the photoemission experiment from the (100) surface probes the Fe bands along the Γ - H high-symmetry line of the bulk Brillouin zone. Assuming, as usual, direct transitions and free-electron final states, only the states intersecting the free-electron parabola shifted by $h\nu=128$ eV (see Fig. 3) are detected in the photoemission spectrum. As one can see from Fig. 3, an excellent agreement between theory and experiment is found. The majority bands are located in two regions, close to the Fermi level and at 4 eV binding energy, while the energy region in between is filled by the minority states at approximately 2.5 eV binding energy. High quality of our films is further confirmed by clear band dispersions in off normal emission at various photon energies (not shown here).

From the band structure shown in Fig. 3, one can see that the Fe 3d states are mostly confined within the first 4 eV below the Fermi energy, while the emission from MgO is mostly at binding energies above 4 eV. This separation between the valence-band emission of the two materials offers, therefore, the opportunity of examining the modifications of the Fe 3d states upon the gradual formation of the Mg/Fe(100) interface.

A representative collection of the valence-band photoemission spectra recorded as a function of MgO deposition is shown in Fig. 4(a). For each coverage, both the spin-resolved components and their sum spectra are shown. For low coverage (0.5, 1, and 2 ML MgO), very little modification is seen in the emission close to E_F (between 0 and 3.5 eV), while the major modification is the appearance of the intense emission centered at approximately 5.5 eV, characteristic of

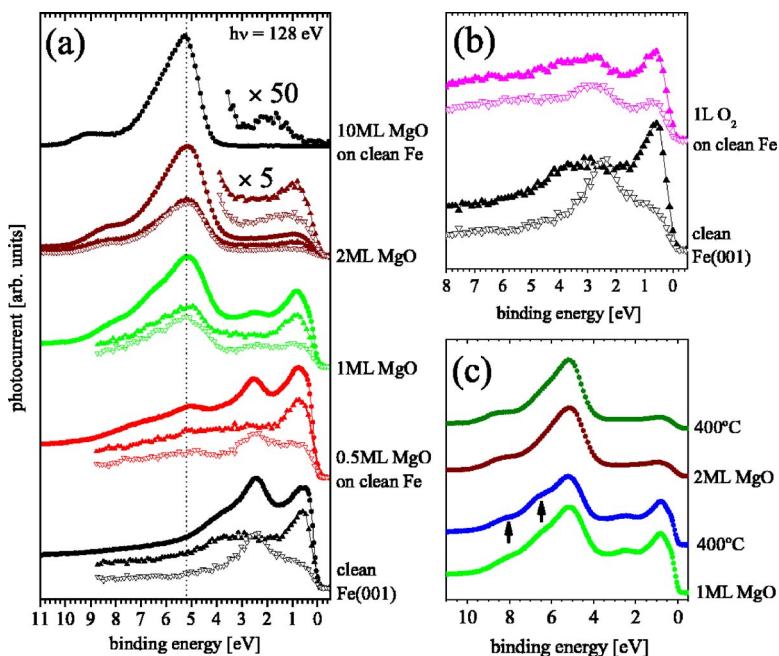


FIG. 4. (Color online) (a) Series of normal emission spin-integrated and spin-polarized spectra of MgO/Fe(001) at $h\nu=128$ eV, (b) comparison of spin-polarized spectra of clean and oxygen-exposed Fe(001), and (c) the effect of 400 °C annealing of 1 and 2 ML MgO/Fe films. The annotations are printed in figure; \blacktriangleright , majority spin; \blacktriangleleft , minority spin. MgO-related features show up at binding energies above 4 eV and are predominantly O 2p character. Spectrum of 10 ML MgO/Fe was taken at 100 K and all other spectra were recorded at room temperature.

highly hybridized O $2p$ and Mg $3s$ of the MgO film.

Clearly, the Fe $3d$ emission close to E_F remains highly spin polarized upon 1 and 2 ML MgO depositions. The MgO features at high binding energy instead are found equally distributed in the spin-up and spin-down channels, indicating that no polarization is induced in the MgO layer.

It is difficult to provide unique interpretation of the small changes observed in the region close to E_F . We observe similar changes at other photon energies (not shown), which is consistent with the study reported by Matthes *et al.*¹⁸ utilizing photon energies of 30–60 eV. Although still clearly dominated by the highly polarized Fe $3d$ states, this region should also contain some emission due to the likely defects within the MgO overlayer. There is a nearly perfect in-plane lattice match between MgO(100) and Fe(100); however, a large number of defects can be expected in the thin film due to the large out-of-plane lattice mismatch (interlayer distances in bulk materials:³² Fe, 1.443 Å; MgO, 2.106 Å). Every terrace boundary in the Fe substrate is, therefore, a source of defects in the MgO overlayer. The presence of defects in the thin films is also consistent with the absence of charging effects in the photoemission experiments from these films. The spectrum obtained from the 10 ML thick MgO film, shown at the top of Fig. 4(a), shows feature assigned to residual defects peaks at about 1.7 eV binding energy. Such a broad unpolarized feature located at this binding energy is, therefore, likely to represent the emission from the MgO defects at low coverage. A spectral feature of this type may explain the modifications observed in the low coverage spectra in the low binding-energy region.

As previously stated, the MgO emission centered at 5.5 eV binding energy is found equally distributed in the spin-up and spin-down channels, offset only by the difference in their respective backgrounds. Theoretical simulations of the electronic band structure of Zhang *et al.*³³ for the MgO/Fe system with an FeO interfacial layer find that the strong hybridization between Fe and O in the FeO layer induces a sizable magnetic moment (as large as $0.19\mu_B$) on the O site of the FeO. Such a large magnetic moment should be reflected in a corresponding large exchange splitting in the O $2p$ band and should be easily detected in the spin-resolved spectra. The experimental results of Fig. 4(a), showing no difference in shape and binding energy between majority and minority spin spectra for low coverage MgO, constitute, therefore, the first strong indication of the absence of interfacial FeO.

It is worth noting that the very small emission in the region close to E_F for the high coverage regime [note the multiplication factor of 50 in the top spectra in Fig. 4(a)] is a clear indication of the high structural quality of these MgO thick films. MgO films thermally evaporated under UHV conditions from stoichiometric MgO source material are indeed known to be nearly stoichiometric or slightly oxygen deficient.³⁴ Theoretical calculations of MgO(100) oxygen deficient surfaces^{35–37} predict wide oxygen vacancy features at 1 eV below the Fermi edge and 2 eV above the valence-band maximum (VBM) of MgO. Such features do not necessarily result from bulk vacancies; they may also result from the intrinsic properties of the MgO surface,³⁵ irregularities, and imperfections of the surface.³⁷ Only weak vacancy features

were present in our spectra at high MgO coverage, as judged by the intensity ratio between the oxygen vacancy and the main O $2p$ feature, being below 0.5% in our films [from Fig. 4(a)] compared to 5% in the spectra from bulk MgO reported by Tjeng *et al.*³⁸ Although these bulk spectra were taken with $h\nu=21.2$ eV (He I lamp), our spectra taken at $h\nu=64$ eV (not shown) still show the ratio to be below 1%. We take this as an indication that our MgO films are grown with good stoichiometry. Another indication comes from the observation of a weak but clear O $2p$ features already at very low MgO coverage (0.5 ML) and at the binding energy equal to one for thicker films.

From the above considerations, it is already quite clear that the Fe(100) surface does not react strongly with the MgO. In order to further address the specific question concerning the formation of an FeO layer at the interface, we have performed additional experiments intentionally exposing the clean Fe surface to small dosages of molecular oxygen. The photoemission spectrum for 1 L (1 L = 10^{-6} Torr s) oxygen exposure is compared with the one from a clean Fe surface in Fig. 4(b). The effect of 1 L oxygen exposure is quite different from the one of the low coverage MgO. Already upon 1 L of oxygen exposure, the spin-up and spin-down spectra tend to assume a similar shape in the Fe $3d$ region, suggesting a depolarization of the surface layer as one would expect when forming FeO.³⁹ This different behavior is, therefore, a second indication of the absence of an FeO layer at the interface.

Finally, an additional point can be learned from the valence-band spectra. In Fig. 4(c), the spin-integrated spectra for 1 and 2 ML MgO/Fe(100) prepared at room temperature and after annealing to 400 °C are compared. All of the room-temperature spectral features are quite broad and so one does not expect major changes from annealing; however, a distinct sharpening of the spectral features is clearly seen, most notably in the fine structure in O $2p$ (see arrows in Fig. 4). The sharpening of the spectral features in angular-resolved photoemission is usually an indication of atomic ordering and reduction of local inhomogeneities.

In Fig. 5, the effects of annealing a 2 ML MgO overlayer are further explored. As already noticed, the deposition of 2 ML of MgO leaves a strong polarization of the Fe-related part of the spectra (above the VBM of MgO), although all the spectral features are broadened by the deposition of the MgO. Annealing these MgO films up to 400 °C begins to sharpen the Fe $3d$ spectral features in the region close to E_F and this process is even more visible in the spectrum annealed at 500 °C, where the sharp spectral feature of the clean Fe surface is nearly fully recovered (see right panel in Fig. 5).

At first sight, this behavior seems to be consistent with a further increase of atomic reordering of the MgO interface at higher temperature. A reordering would certainly correspond to a decreased emission from MgO defects in the region of the Fe $3d$. Furthermore, the electrons excited in the Fe underneath MgO would leave the surface with less scattering if the crystalline structure of the interface is improved and this would explain both the reappearance of the sharp Fe features and the decrease in the intensity ratio of O $2p$ to Fe-related parts of spectra.

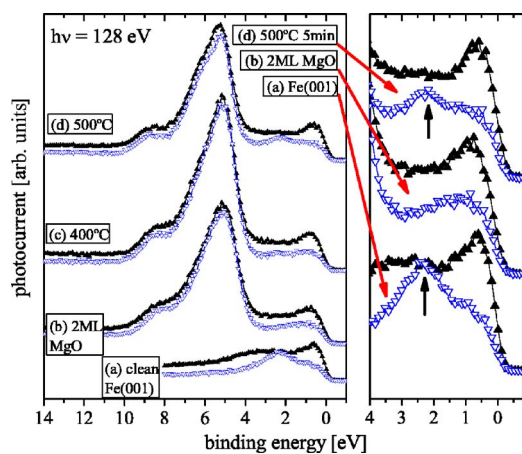


FIG. 5. (Color online) Spin-polarized photoemission spectra at $h\nu=128$ eV; \blacktriangle , majority spin; \blacktriangledown , minority spin. Left panel: (a) clean Fe(100) and (b) 2 ML of MgO/Fe(100) (c) annealed to 400 °C for 5 min and (d) subsequently annealed to 500 °C for 5 min. In right panel, selected spectra are magnified in the region close to the Fermi edge. Spectra are normalized to the majority spin Fe-related part near the Fermi edge. All spectra were taken at room temperature.

We cannot, however, exclude also the possibility that the recovering of the sharp Fe 3*d* feature could be due to partial uncovering of the bare Fe surface by clustering and/or desorption of the MgO. After all, MgO molecules must have some degree of mobility at high temperature if reordering is affected. Furthermore, this hypothesis would also naturally explain the decrease in the intensity ratio of O 2*p* to Fe-related parts of the spectra in Fig. 5(d), compared to the constant ratio in Figs. 5(b) and 5(c). Finally, this interpretation would also explain the degradation of the magnetic tunneling properties experimentally observed for temperatures just above 400 °C.³

In summary, on the important topic of the temperature stability of the MgO/Fe interface, the photoemission data do not offer a complete answer. The two different models presented above would seem to be both consistent with the present observations, although they would have quite different implications for the fabrication of high-quality MTJs. A way to sort out this question would possibly be to perform microscopy studies on this system.

B. Fe 3*p* and Mg 2*p* core-level measurements

We now turn to the study of the shallow Fe and Mg core levels. As mentioned above, at the photon energy of 128 eV, one can simultaneously excite both the Fe 3*p* and the Mg 2*p* levels. These core levels are located at binding energies of 53 and 51 eV, respectively, and, although quite close, they still offer the possibility of monitoring the two different materials during the formation of the interface. Furthermore, the Fe 3*p* levels exhibit a large magnetic linear dichroism in photoemission,⁴⁰ which can be used to monitor the magnetic state of the Fe layer. The core-level data are displayed in Fig. 6, where results concerning the growth and annealing of MgO layers on top of Fe(001) surface are shown, similar to

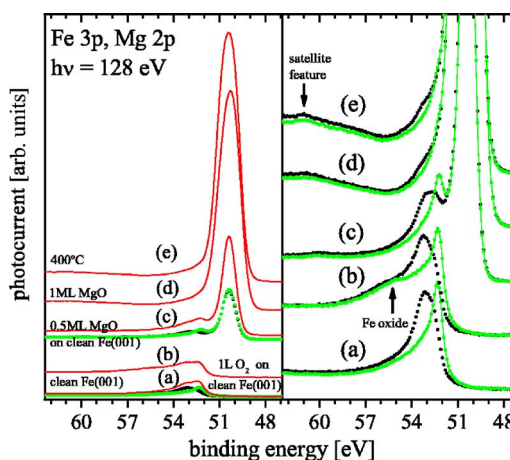


FIG. 6. (Color online) Fe 3*p* and Mg 2*p* core-level normal emission energy distribution curves at $h\nu=128$ eV; (a) clean Fe(001), (b) Fe(001) exposed to 1 L of molecular oxygen, (c) 0.5 ML MgO/Fe(001) deposited on clean Fe(001), (d) 1 ML MgO/Fe(001), and (e) previous films annealed to 400 °C for 5 min. In the left panel, the sum of spectra from the sample magnetized in opposite directions is plotted. The right panel shows the same spectra as on the left but renormalized to magnify the Fe 3*p* contribution. Opened and closed circles represent spectra from the sample magnetized in opposite directions. All spectra were measured at room temperature.

the study utilizing the valence-band photoemission already discussed. The left panel presents mostly dichroic averaged spectra (continuous lines), while the right panel shows the corresponding dichroism spectra (open and closed circles), in an expanded view emphasizing the smaller region around the Fe 3*p* levels.

Comparing the spectra from the clean Fe(100) surface [Fig. 6(a)] to the ones exposed to 1 L of molecular oxygen [Fig. 6(b)], the appearance of a shoulder on the high binding-energy side of the spectrum is evident. This shoulder feature, best seen in the right panel of Fig. 6, is typical of the reaction of oxygen with Fe and indicates the formation of Fe oxide.⁴¹ In agreement with the valence-band observations, this shoulder does not display any dichroism, indicating the formation of an unpolarized surface oxide upon even 1 L of oxygen exposure to the clean Fe surface. Most importantly, when MgO is deposited on clean Fe(001) instead [Fig. 6(c)], there is no indication of this feature in the spectra. On the contrary, the curvature of the relevant part of the core-level spectrum remains clearly positive for 1 ML MgO coverage, which is further evidence that no FeO layer is present at the MgO(100)/Fe(100) interface.

At higher MgO deposition, the Fe 3*p* emission becomes rapidly obscured by the much more intense Mg 2*p* levels [Figs. 6(c) and 6(d)] but the Fe dichroism remains strong, which indicates a highly polarized Fe substrate in contact with the MgO overlayer. It is also useful to note that while the Fe dichroism is very strong, no sign of any dichroism is detected under the Mg peak (the full dichroic spectra are shown in the left panel for the case 0.5 ML MgO, as an example). This again tends to confirm the low interaction between Fe and MgO at the interface.

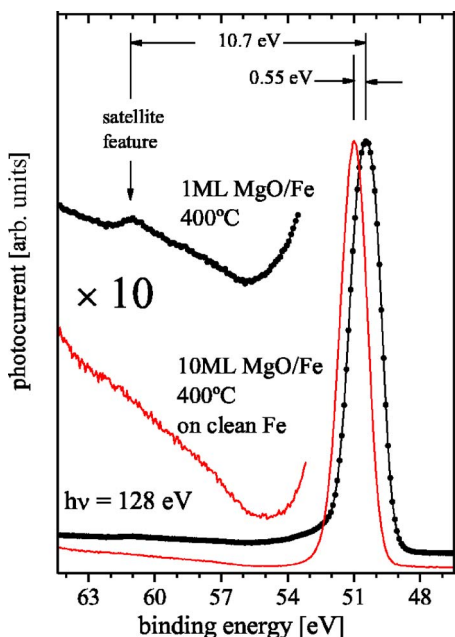


FIG. 7. (Color online) Core-level and small satellite feature spectra of MgO/Fe(100). Full circles, 400 °C 1 ML MgO/Fe; solid line, 400 °C 10 ML MgO/Fe. Spectrum of 1 ML coverage was measured at room temperature and the 10 ML spectrum at 100 K. Renormalized parts of spectra are also shown.

For the thicker films where no Fe signal remains, there is no additional Mg 2*p* line related to metallic Mg. Such a metallic feature would be expected to appear at 2 eV lower binding energy from the main 2*p* line of MgO (Ref. 42) and its complete absence is, therefore, a further confirmation of the good stoichiometry of these films. In agreement to what was found in the valence-band study, when annealing MgO/Fe(100) interface to 400 °C [Fig. 6(e)], there is little change in the core level with only the shape of the Mg 2*p* spectra becomes slightly more symmetrical. However, most interestingly, upon annealing the 1 ML MgO/Fe(001) a small feature, which is barely visible in the RT-deposited MgO, clearly appears at 10.7 eV above the Mg 2*p* binding energy (this is best seen in Fig. 7 and further discussed below) but, quite independently of the precise interpretation, the observed sharpening of the features indicates again a structural reordering of the MgO layer induced by annealing.

Finally, we provide a brief analysis of the effects related to the fast response of the Fe substrate to photoexcitation in the MgO film. Two effects observed are shown in Fig. 6, where a comparison of Mg 2*p* spectra of 1 ML MgO and 10 ML MgO film on Fe(100), both annealed to 400 °C, is made. First, we focus on the interface-induced electron screening as observed in the Mg 2*p* spectra of thin MgO layer in contact with the Fe substrate. Figure 7 shows that there is substantial shift of Mg 2*p* (0.55 eV) to lower binding energy for thin MgO layer. This shift occurs gradually with increasing coverage, and was routinely reproduced over many freshly prepared MgO/Fe(100) films (not shown). Such shift is in agreement with previous results from other MgO/metal interfaces.^{43,44} The interpretation of the energetics of the photoemission process in strongly correlated materials in the

immediate presence of metallic layers, which can rapidly respond to the photoemission process, has been presented by Duffy and Stoneham⁴⁵ and in references therein. More recently, related x-ray photoemission experiments performed by Altieri *et al.*^{43,44} for the case of the MgO/Ag(100) interface showed a shift of the Mg 2*p* peak on the order of 1 eV with increasing MgO coverage, which was ascribed to image potential screening from the underlying metal substrate. In other words, while the charge relaxation in MgO appears to be slow on the time scale of the photoemission process, the screening of the hole created in the photoemission process by underlying metal is rapid on this time scale. In this way, the presence of the metal substrate influences the energy of the photoelectron emitted from as far as 10 ML away from the interface.⁴³ In this interpretation, the observed shift can be different for various core-level and valence-band features due to different screening effects. We clearly observe such effect in Fig. 7, and it is not due to charging, since no substantial shift between thin and thick MgO layers is observed in the O 2*p* part of the valence band [Fig. 4(a)]. This is in contrast to MgO films with higher thicknesses (≥ 15 ML), where charging effects are clearly detected in photoemission spectra. The absence of charging effects in thinner MgO might be a result of efficient tunneling from the Fe substrate. The observed interfacial screening reveals the dynamics of electronic response at the metal and/or insulator interface that could be relevant in tunneling.

The second interesting observation that can be made from Fig. 7 is an appearance of small feature at about 10.7 eV below the Mg 2*p* peak in the spectrum for 1 ML MgO/Fe(100). This feature is completely absent in the clean Fe spectrum and it also disappears for thick MgO films. Furthermore, we note that this feature is barely visible in the RT-deposited 1 ML MgO film [see Fig. 6(d)], and it is enhanced significantly by annealing to 400 °C [see Fig. 7 and also Fig. 6(e)]. It also appears to be diminished in strength for submonolayer MgO coverage, as seen for the 0.5 ML MgO spectrum [Fig. 6(c)]. We suggest that this feature is another example of a response of a conduction electrons of the Fe underlayer to the excitation produced in the MgO overlayer. Full support to this interpretation is given by the fact that Fe surface plasmon peak is reported to be at energy loss of 10–11 eV by previous studies.^{46,47} Thus, we assign the feature observed at 10.7 eV below the Mg 2*p* to a plasmon excited in the Fe interface by sudden creation of the core hole in the MgO layer across the insulator and/or metal interface. Such plasmon feature excited across the metal and/or insulator interfaces was reported recently for MgO/Ag system,⁴⁸ where it is also demonstrated that the exact energy of such plasmon is shifted from the value for a clean surface due to the changes of the electronic structure at the interface. The energy shift for that system is reported to be on the order of a fraction of an eV which is fully consistent with our observation. In conclusion, the observation of the Fe surface plasmon in the Mg 2*p* spectrum is another indication of nontrivial electronic dynamics at the metal and/or insulator interface.

IV. SUMMARY

The electronic structure of epitaxial MgO(100) films grown on Fe(100) has been investigated by valence-band

spin-polarized photoemission and shallow core-level spectroscopy. The deposition of epitaxial MgO overlayers has been realized by direct evaporation of stoichiometric MgO on Fe(100) at room temperature. The good structural and compositional quality of these MgO films was confirmed by the small photocurrent intensity observed above the valence-band maximum for the 10 ML film coverage and by the absence of a metallic component in the Mg $2p$ spectrum. From the valence-band spectra, the Fe $3p$, and the Mg $2p$ spectra, no indications of an FeO layer were found at the MgO/Fe(100) interface prepared in this way. The high spin polarization of the Fe valence band above the VBM of MgO is preserved in the low coverage range and only a small reduction in the sharpness of the Fe $3d$ features is observed. Annealing the interface to 400 °C only partially restores the sharpness of the Fe $3d$ features, very probably as a result of structural ordering of the interface. Annealing to 500 °C influences more strongly both the Fe- and MgO-related parts of the spectra. The recovery of the full sharpness of the Fe $3d$ features could be the result of further and more complete ordering of the interface or to uncovering the clean Fe(100)

substrate. No unambiguous interpretation can be offered on this point from our data but a microscopy study should be able to resolve the ambiguity.

In addition, we report several interesting electronic properties of the interface by comparing the core-level spectra at various MgO coverages. The binding energy of the Mg $2p$ levels increases by 0.55 between 1 and 10 ML coverages. At 1 ML coverage, a small feature is present at a binding energy of 10.7 eV below the main Mg $2p$ line; it is ascribed to a plasmon deexcitation from the underlying Fe substrate.

ACKNOWLEDGMENTS

We would like to thank the NSLS staff for the technical support on the course of experiments. This work was supported by NSF Grant No. ECS-0300235. The National Synchrotron Light Source, Brookhaven National Laboratory, is supported by the U.S. Department of Energy, Office of Science, Office of Basic Energy Sciences, under Contract No. DE-AC02-98CH10886.

*Electronic address: plucinski@phys.uconn.edu

¹W. H. Butler, X.-G. Zhang, T. C. Schulthess, and J. M. MacLaren, *Phys. Rev. B* **63**, 054416 (2001).

²J. Mathon and A. Umerski, *Phys. Rev. B* **63**, 220403(R) (2001).

³S. S. P. Parkin, C. Kaiser, A. Panchula, P. M. Rice, B. Hughes, M. Samant, and S.-H. Yang, *Nat. Mater.* **3**, 862 (2004).

⁴S. Yuasa, T. Nagahama, A. Fukushima, Y. Suzuki, and K. Ando, *Nat. Mater.* **3**, 868 (2004).

⁵S. Yuasa, T. Katayama, T. Nagahama, A. Fukushima, H. Kubota, Y. Suzuki, and K. Ando, *Appl. Phys. Lett.* **87**, 222508 (2005).

⁶J. Hayakawa, S. Ikeda, F. Matsukura, H. Takahashi, and H. Ohno, *Jpn. J. Appl. Phys., Part 2* **44**, L587 (2005).

⁷S. Ikeda, J. Hayakawa, Y. M. Lee, T. Tanikawa, F. Matsukura, and H. Ohno, *J. Appl. Phys.* **99**, 08A907 (2006).

⁸H. L. Meyerheim, R. Popescu, J. Kirschner, N. Jedrecy, M. Sauvage-Simkin, B. Heinrich, and R. Pinchaux, *Phys. Rev. Lett.* **87**, 076102 (2001).

⁹C. Tiusan, J. Faure-Vincent, C. Bellouard, M. Hehn, E. Jouguelet, and A. Schuhl, *Phys. Rev. Lett.* **93**, 106602 (2004).

¹⁰K. Miyokawa, S. Saito, T. Katayama, T. Saito, T. Kamino, K. Hanashima, Y. Suzuki, K. Mamiya, T. Koide, and S. Yuasa, *Jpn. J. Appl. Phys., Part 2* **44**, L9 (2005).

¹¹P. Luches, S. Benedetti, M. Liberati, F. Boscherini, I. Pronin, and S. Valeri, *Surf. Sci.* **583**, 191 (2005).

¹²M. Sicot, S. Andrieu, F. Bertran, and F. Fortuna, *Phys. Rev. B* **72**, 144414 (2005).

¹³C. Li and A. J. Freeman, *Phys. Rev. B* **43**, 780 (1991).

¹⁴B. D. Yu and J.-S. Kim, *Phys. Rev. B* **73**, 125408 (2006).

¹⁵J. Mathon and A. Umerski, *Phys. Rev. B* **71**, 220402(R) (2005).

¹⁶K. D. Belashchenko, J. Velev, and E. Y. Tsymlal, *Phys. Rev. B* **72**, 140404(R) (2005).

¹⁷R. Wang, X. Jiang, R. M. Shelby, R. M. Macfarlane, S. S. P. Parkin, S. R. Bank, and J. S. Harris, *Appl. Phys. Lett.* **86**, 052901 (2005).

¹⁸F. Matthes, L.-N. Tong, and C. M. Schneider, *J. Appl. Phys.* **95**, 7240 (2004).

¹⁹M. Sicot, S. Andrieu, P. Turban, Y. Fagot-Revurat, H. Cercellier, A. Tagliaferri, C. DeNadai, N. B. Brookes, F. Bertran, and F. Fortuna, *Phys. Rev. B* **68**, 184406 (2003).

²⁰M. Sicot, S. Andrieu, P. Turban, Y. Fagot-Revurat, H. Cercellier, A. Tagliaferri, C. Denadai, N. B. Brookes, F. Bertran, and F. Fortuna, *IEEE Trans. Magn.* **40**, 2305 (2004).

²¹Y. S. Dedkov, M. Fonin, U. Rüdiger, and G. Güntherodt, *Appl. Phys. A: Mater. Sci. Process.* **82**, 489 (2006).

²²T. T. Magkoev, G. G. Vladimirov, D. Remar, and A. M. C. Moutinho, *Solid State Commun.* **122**, 341 (2002).

²³E. Vescovo, H.-J. Kim, Q.-Y. Dong, G. Nintzel, D. Carlson, S. Hulbert, and N. V. Smith, *Synchrotron Radiat. News* **12**, 10 (2004).

²⁴EA125, Omicron NanoTechnology GmbH.

²⁵G. C. Burnett, T. J. Monroe, and F. B. Dunning, *Rev. Sci. Instrum.* **65**, 1893 (1994).

²⁶E. Bauer, *J. Phys.: Condens. Matter* **11**, 9365 (1999).

²⁷Z. Q. Qiu, J. Pearson, A. Berger, and S. D. Bader, *Phys. Rev. Lett.* **68**, 1398 (1992).

²⁸P. J. Berlowitz, J. W. He, and D. W. Goodman, *Surf. Sci.* **231**, 315 (1990).

²⁹W. Wulfhekel, F. Zavaliche, R. Hertel, S. Bodea, G. Steierl, G. Liu, J. Kirschner, and H. P. Oepen, *Phys. Rev. B* **68**, 144416 (2003).

³⁰K. von Bergmann, M. Bode, A. Kubetzka, O. Pietzsch, and R. Wiesendanger, *Microsc. Res. Tech.* **66**, 61 (2005).

³¹M. Klaua, D. Ullmann, J. Barthel, W. Wulfhekel, J. Kirschner, R. Urban, T. L. Monchesky, A. Enders, J. F. Cochran, and B. Heinrich, *Phys. Rev. B* **64**, 134411 (2001).

³²H. L. Meyerheim, R. Popescu, N. Jedrecy, M. Vedpathak, M. Sauvage-Simkin, R. Pinchaux, B. Heinrich, and J. Kirschner, *Phys. Rev. B* **65**, 144433 (2002).

- ³³X.-G. Zhang, W. H. Butler, and A. Bandyopadhyay, *Phys. Rev. B* **68**, 092402 (2003).
- ³⁴J. L. Vassent, A. Marty, B. Gilles, and C. Chatillon, *J. Cryst. Growth* **219**, 434 (2000).
- ³⁵L. Giordano, J. Goniakowski, and G. Pacchioni, *Phys. Rev. B* **64**, 075417 (2001).
- ³⁶F. Finocchi, J. Goniakowski, and C. Noguera, *Phys. Rev. B* **59**, 5178 (1999).
- ³⁷L. N. Kantorovich, J. M. Holender, and M. J. Gillan, *Surf. Sci.* **343**, 221 (1995).
- ³⁸L. H. Tjeng, A. R. Vos, and G. A. Sawatzky, *Surf. Sci.* **235**, 269 (1990).
- ³⁹It is worth noting that Bertacco and Ciccacci, *Phys. Rev. B* **59**, 4207 (1999), suggest that ordered overlayers of oxygen enhance spin polarization in inverse photoemission of Fe(100).
- ⁴⁰C. Roth, F. U. Hillebrecht, H. B. Rose, and E. Kisker, *Phys. Rev. Lett.* **70**, 3479 (1993).
- ⁴¹B. Sinkovic, P. D. Johnson, N. B. Brookes, A. Clarke, and N. V. Smith, *J. Appl. Phys.* **70**, 5918 (1991).
- ⁴²M. Kurth, P. C. J. Graat, and E. J. Mittemeijer, *Appl. Surf. Sci.* **220**, 60 (2003).
- ⁴³S. Altieri, L. H. Tjeng, F. C. Voogt, T. Hibma, and G. A. Sawatzky, *Phys. Rev. B* **59**, R2517 (1999).
- ⁴⁴S. Altieri, L. Tjeng, and G. Sawatzky, *Thin Solid Films* **400**, 9 (2001).
- ⁴⁵D. M. Duffy and A. M. Stoneham, *J. Phys. C* **16**, 4087 (1983).
- ⁴⁶Y. Sakisaka, T. Miyano, and M. Onchi, *Phys. Rev. B* **30**, 6849 (1984).
- ⁴⁷B. Egert and G. Panzner, *J. Phys. F: Met. Phys.* **11**, L233 (1981).
- ⁴⁸S. Altieri, L. H. Tjeng, F. C. Voogt, T. Hibma, O. Rogojuanu, and G. A. Sawatzky, *Phys. Rev. B* **66**, 155432 (2002).
- ⁴⁹P. Blaha, K. Schwarz, G. K. H. Madsen, D. Kvasnicka, and J. Luitz, *An Augmented Plane Wave+Local Orbitals Program for Calculating Crystal Properties* (Technische Universität Wien, Austria, 2000).